Earth and Planetary Science Letters 369–370 (2013) 1–12

Contents lists available at SciVerse ScienceDirect

Earth and Planetary Science Letters

journal homepage: www.elsevier.com/locate/epsl

Neogene rejuvenation of central Appalachian topography: Evidence for differential rock uplift from stream profiles and erosion rates

Scott R. Miller [a,*], Peter B. Sak [b], Eric Kirby [c,d], Paul R. Bierman [e]

[a] Department of Earth and Environmental Sciences, University of Michigan, Ann Arbor, MI 48109, USA
[b] Department of Earth Sciences, Dickinson College, Carlisle, PA 17013, USA
[c] Department of Geosciences, Pennsylvania State University, University Park, PA 16802, USA
[d] Institute for Earth and Environmental Sciences, University of Potsdam, Potsdam, Germany
[e] Department of Geology, University of Vermont, Burlington, VT 05405, USA

ARTICLE INFO

Article history:
Received 15 November 2012
Received in revised form
6 April 2013
Accepted 6 April 2013
Editor: T.M. Harrison
Available online 11 May 2013

Keywords:
Appalachian Mountains
stream profile
knickpoint
transient erosion
cosmogenic nuclides

ABSTRACT

The persistence of topography within ancient orogens remains one of the outstanding questions in landscape evolution. In the eastern North American Appalachians, this question is manifest in the outstanding problem of whether topographic relief is in a quasi-equilibrium state, decaying slowly over many millennia, or whether relief has increased during the late Cenozoic. Here we present quantitative geomorphic data from the nonglaciated portion of the Susquehanna River drainage basin that provide insight into these end-member models. Analysis of channel profiles draining upland catchments in the northern Valley and Ridge, Appalachian Plateau, Blue Ridge, and Piedmont provinces reveals that a large number of streams have well defined knickpoints clustered at 300–600 m elevation but not systematically associated with transitions from weak to resistant substrate. Cosmogenic ^{10}Be inventories of modern stream sediment indicate that erosion rates are spatially variable, ranging from ∼5–30 m/Myr above knickpoints to ∼50–100 m/Myr below knickpoints. Overall, channel gradients, normalized for drainage area, scale linearly with catchment-averaged erosion rates. Collectively, regionally consistent spatial relationships among erosion rate, channel steepness, and knickpoints reveal an ongoing wave of transient channel adjustment to a change in relative base level. Reconstructions of relict channel profiles above knickpoints suggest that higher rates of incision are associated with ∼100–150 m of relative base level fall that accompanied epierogenic rock uplift rather than a change to a more erosive climate or drainage reorganization. Channel response timescales imply that the onset of relative base level change predates ∼3.5 Ma and may have begun as early as ∼15 Ma. We suggest that adjustment of the channel network was likely driven by changes in mantle dynamics along the eastern seaboard of North America during the Neogene.

1. Introduction

Despite significant progress in understanding the coupling among topography, climate, and tectonics within active orogens (Whipple, 2009), the persistence of topography observed along many passive margins remains enigmatic (Baldwin et al., 2003; Bishop and Goldrick, 2010; Scharf et al., 2013). As an example, the eastern seaboard of North America has been a passive continental margin for ∼180 Myr (Faill, 1998); yet, the Appalachian Mountains retain significant topographic relief, with the highest elevations reaching just over 2000 m above sea level (Fig. 1A). The history of this topography has long been a topic of study (Davis, 1889), and a continuing debate centers on whether Appalachian topography is in a state of quasi-equilibrium (e.g., Hack, 1960; Matmon et al., 2003), maintained isostatically but decaying slowly over geologic time (e.g., Baldwin et al., 2003), or whether it has been rejuvenated during the late Cenozoic (e.g., Davis, 1889; Hack, 1982; Poag and Sevon, 1989; Hancock and Kirwan, 2007; Gallen et al., 2013; Portenga et al., 2013; Prince and Spotila, in press).

Recent geomorphic studies in the Appalachians have revealed fluctuations in channel incision during late Cenozoic time (Poag and Sevon, 1989; Pazzaglia and Gardner, 1993; Sasowsky et al., 1995; Granger et al., 1997; Springer et al., 1997; Reusser et al., 2004; Ward et al., 2005), that stand in apparent contradiction to the conventional wisdom that slow degradation of topography has been sustained for >100 Myr (Matmon et al., 2003; Spotila et al., 2004). Potential drivers of erosion rate variability, however, remain a point of debate, with workers alternatively favoring climate change (Boettcher and Milliken, 1994; Reusser et al., 2004; Ward et al., 2005; Hancock and Kirwan, 2007; Westaway,

* Corresponding author.
E-mail address: srmill@umich.edu (S.R. Miller).

0012-821X/$ - see front matter © 2013 Elsevier B.V. All rights reserved.
http://dx.doi.org/10.1016/j.epsl.2013.04.007

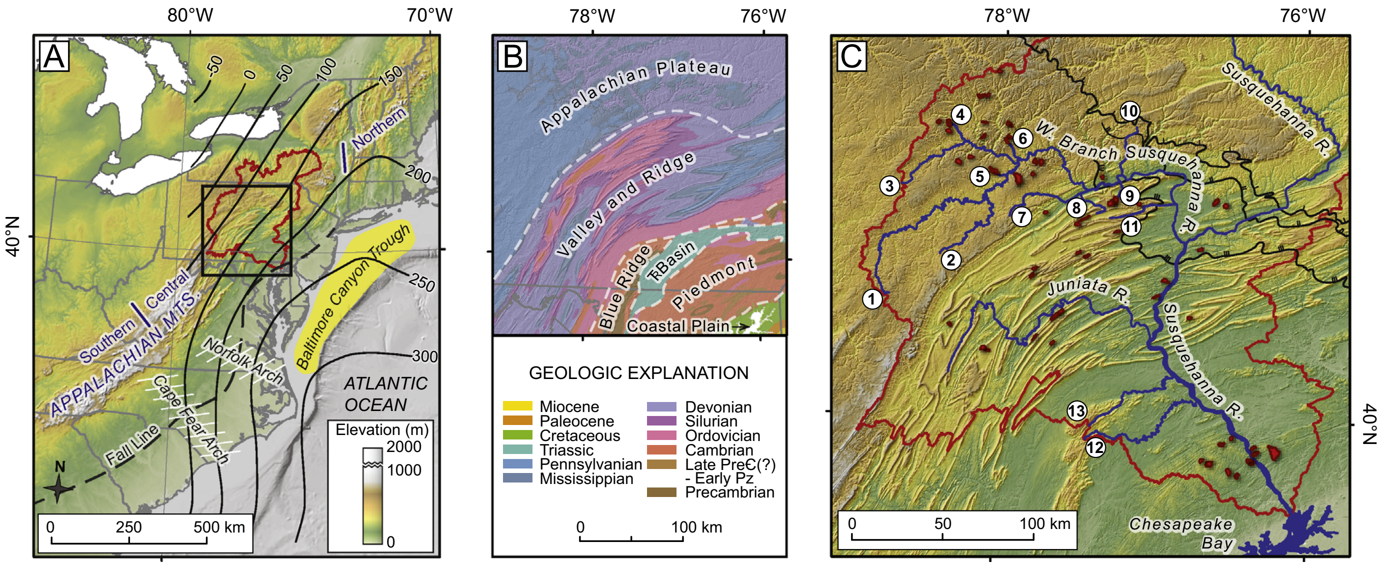

Fig. 1. Maps of study area. (A) Digital elevation model (DEM) of the eastern USA showing the Appalachian Mountains, Susquehanna River catchment (red), and Baltimore Canyon Trough (yellow). Black contours show change in dynamic topography since 30 Ma, in meters (modified from Moucha et al. (2008)). Dashed line is the Fall Line. Location of panels B and C outlined in black. (B) Geologic map draped over shaded relief DEM of study area. Geologic province boundaries shown with white dashed lines. (C) Red polygons mark individual catchments used in erosion rate and stream profile analyses. Black lines mark southern margins of major glacial advances from Fullerton et al. (2003)) (one tic: late Wisconsin; two tics: Illinoian; three tics: pre-Illinoian). Thick blue lines mark streams referred to in text and other figures (1: W. Branch Susquehanna R.; 2: Moshannon Ck.; 3: Bennett Branch Sinnemahoning Ck.; 4: E. Branch Hicks Run; 5: Little Birch Island Run; 6: Lebo Branch Cooks Run; 7: N. Fork Beech Ck.; 8: Long Run; 9: Gottshall Run; 10: Larrys Ck.; 11: White Deer Ck.; 12: W. Conewago Ck.; 13: Mountain Ck.). (For interpretation of the references to color in this figure legend, the reader is referred to the web version of this article.)

2007), drainage reorganization and stream capture (Harbor et al., 2005; Pazzaglia et al., 2006; Gunnell and Harbor, 2010; Prince et al., 2010, 2011; Prince and Spotila, in press), or changes in the tectonic rock uplift rate (Poag and Sevon, 1989; Pazzaglia and Brandon, 1996; Gallen et al., 2013).

Lately, studies of density-driven flow in the mantle (Moucha et al., 2008; Spasojević et al., 2008) have renewed interest in dynamically supported topography along the eastern North American margin (Vogt, 1991; Pazzaglia and Brandon, 1996; King, 2007), perhaps associated with intraplate seismicity in the region (Wolin et al., 2012). Although important differences among models and their predictions exist (Flament et al., 2013), such models provide reasonable explanations for anomalous sea-level curves determined from the Atlantic passive margin (Spasojević et al., 2008) and deformed shorelines across the Cape Fear and Norfolk Arches (Rowley et al., 2011). Moreover, some model realizations (Moucha et al., 2008) raise the possibility that changes in mantle circulation since ~30 Ma have driven surface uplift of ~100–200 m inboard of the coastal margin (Fig. 1A). Although such changes should, in principle, be measurable, the scarcity of geomorphic markers with which to gauge subtle, long-wavelength deformation in the eroding upland landscapes of the Appalachians, and thus test dynamic topography models, makes this challenging.

River profiles are increasingly exploited as gauges of tectonic and climate change (Wobus et al., 2010; Kirby and Whipple, 2012; Schildgen et al., 2012). Interpretations of profile shape are complicated where rivers cross substrates with contrasting erodibilities because equilibrium channel gradients depend on rock mass quality and resistance to erosion (e.g., Duvall et al., 2004). Such complications are present in the Appalachians, where the Paleozoic fold and thrust belt structure is clearly displayed in the topography (Hack, 1960; Mills, 2003). Consequently, it has been difficult in the Appalachians to show whether knickpoints in river profiles—traditional geomorphic fingerprints of perturbations in incision rate (e.g., Bishop et al., 2005)—are migratory, reflecting changes in external forcing, or whether these are stable, anchored by spatial variations in substrate erodibility (Hickok, 1933; Morisawa, 1962; Harbor et al., 2005; Frankel et al., 2007; Gallen et al., 2011, 2013; Prince et al., 2011; Prince and Spotila, in press). Central to this problem, it remains to be shown in the Appalachians that knickpoints thought to be migratory (e.g., Gallen et al., 2013; Prince and Spotila, in press) correspond to along-stream variations in incision rate.

In this paper, we examine whether the topography in the Susquehanna River drainage basin (Fig. 1), part of the central Appalachian Mountains, can be considered in a steady state or whether it records the imprint of transient channel incision. Because this region is largely upstream of relict fluvial terraces (Pazzaglia and Gardner, 1993), we combine quantitative analyses of channel longitudinal profiles (Wobus et al., 2006a; Kirby and Whipple, 2012) with existing determinations of erosion rate from in-situ cosmogenic ^{10}Be inventories in fluvial sediment (Reuter, 2005; Portenga and Bierman, 2011). The results demonstrate that regional channel gradients and erosion rates are adjusting to 100–150 m of base level fall that most likely began in the Neogene. Finally, we explore the implications of our results for geodynamic predictions of mantle-driven late Cenozoic surface uplift. Our results demonstrate that stream profile analyses coupled with basin-averaged erosion rate data provide a powerful tool for detecting and quantifying transient erosion in a lithologically diverse, ancient orogen.

2. Study area

The 71,200 km^2 catchment of the Susquehanna River is the largest draining the eastern slope of the Appalachians. Our study focuses on the part of that catchment that is south of the limit of Quaternary glaciation and mostly within the state of Pennsylvania, USA (Fig. 1). Elevations range from sea level to 957 m. This region encompasses a part of the Paleozoic Appalachian orogen that was rifted locally during the Triassic and has subsequently become the North American passive margin (Faill, 1998, 2003). Today, the area comprises six geologic and physiographic provinces (Fig. 1B) with varying bedrock geology, structure, and topographic relief (Schultz, 1999). Farthest upstream, the Appalachian Plateau province consists of flat-lying to gently folded Paleozoic clastic rocks (shale, sandstone, and conglomerate) and has up to 400 m of local relief, measured in a 2.5 km radius window. The Valley and Ridge province (≤400 m relief) is made up largely of folded Paleozoic carbonate, shale, sandstone, and quartzite. The Piedmont (≤200 m relief) and Blue Ridge (≤300 m relief) provinces are underlain by Precambrian to early Paleozoic crystalline rocks. Only in the Piedmont have stream terraces been documented that are thought to be older than the Pleistocene (Pazzaglia and Gardner, 1993; Engel et al., 1996). The Triassic Gettysburg basin (≤200 m relief) is largely igneous and lacustrine sedimentary rocks. At its mouth, the Susquehanna River crosses the physiographic Fall Line that marks the contact between the Piedmont and onlapping Cretaceous to Cenozoic Coastal Plain sediments.

3. Methods

3.1. Stream profile analysis

Stream profile analysis (Wobus et al., 2006a; Kirby and Whipple, 2012) is based on the relationship between channel gradient and erosion rate, both of which adjust to rock uplift, climate, and lithology (Duvall et al., 2004; DiBiase and Whipple, 2011). This relationship is supported by a growing body of empirical work from active orogens that demonstrates that channel steepness increases monotonically with catchment-averaged erosion rate averaged over 10^3–10^5 yr timescales (Kirby and Whipple, 2001; Safran et al., 2005; Wobus et al., 2006a; Harkins et al., 2007; Ouimet et al., 2009; Cyr et al., 2010; DiBiase et al., 2010).

Stream profile analysis accounts for the fact that channel gradients along a stream course commonly exhibit an inverse power-law scaling relationship with contributing drainage area, associated with graded, concave-up stream profiles (Flint, 1974). This scaling relationship is defined by two parameters that are estimated by least-squares linear regression of log-slope and log-area: a concavity index, θ, and a steepness index, k_s (see Online supplementary materials). The latter parameter can be an effective metric with which to compare the slopes of channels, normalizing for differences in basin shape and drainage area. To facilitate comparison among streams, it is common practice to calculate a normalized steepness index, k_{sn}, using a fixed reference concavity, θ_{ref} (e.g., Snyder et al., 2000; Kirby et al., 2003). Although similar to methods that rely on slope–distance relationships (Goldrick and Bishop, 2007) and that compare channel slopes at a reference drainage area (Sklar and Dietrich, 1998), this method has the advantage of being more flexible when comparing among streams of widely different size and with different catchment shapes (see discussion in Kirby and Whipple (2012)).

Although stream profile analysis was developed in the context of steady state landscapes (those where incision balances uplift of rock), it has been extended to transient systems as well (e.g., Schoenbohm et al., 2004; Clark et al., 2005; Harkins et al., 2007; Kirby et al., 2007; Kirby and Whipple, 2012; Miller et al., 2012; Morell et al., 2012; Olivetti et al., 2012; Schildgen et al., 2012; Walcek and Hoke, 2012). When rock uplift rate increases, for example, channels respond by steepening profile gradients. In detachment-limited (bedrock) streams, this adjustment begins downstream and migrates upstream until the entire channel is adjusted to the new boundary condition (Whipple and Tucker, 1999). The point or reach separating gentler channel gradients upstream from steeper gradients downstream is the knickpoint or knickzone, readily identified both on longitudinal profiles and also as abrupt downstream increases in steepness index on plots of log-slope against log-area (Wobus et al., 2006b). However, distinguishing transient or migratory knickpoints from stable knickpoints anchored to resistant substrate requires knowledge of underlying geology as well as independent determinations of erosion rates above and below the knickpoints (e.g., Harkins et al., 2007).

We analyzed stream profiles using a US National Elevation Dataset DEM (Gesch, 2007; accessed July 2009) with 1/3-arc-second resolution that we projected to a Universal Transverse Projection and cell size of 10 m. Slope and drainage area were calculated at a 12.2 m elevation interval, the contour interval (40 ft) of the data from which the DEM was partially derived. Fifty-six small tributary catchments, 0.6–25.3 km^2 in area and ranging from low to high local relief, were chosen to study the relationship between channel steepness and erosion rate, which provides details about stream profile dynamics on a local scale. Each catchment is underlain by a single dominant lithology, either shale, sandstone, quartzite, or schist, as categorized by Miles and Whitfield (2001). For each catchment, we calculated the mean k_{sn} following the procedure of Ouimet et al. (2009) using the 10 m resolution DEM and setting θ_{ref}=0.45 (Fig. 1C; see Online supplementary materials for further details).

For a larger-scale analysis that places these individual catchments in a regional context, we downsampled the DEM to 90 m resolution for computational feasibility. For this part of the study, we inspected the profiles of 60 individual tributaries, estimating concavity and normalized steepness indices (θ_{ref}=0.45) and mapping knickpoints where channel profiles steepen by a factor of >2 and exhibit offset trends in slope-area scaling. Knickpoint locations were compared to Pennsylvania's 1:250,000-scale digital map of bedrock geology in order to assess the role of lithology (Miles and Whitfield, 2001).

3.2. Catchment-averaged erosion rates

For each of the 56 small catchments, erosion rates were determined from cosmogenic ^{10}Be measured in quartz extracted from river sand in active channels (Brown et al., 1995; Bierman and Steig, 1996; Granger et al., 1996; Bierman and Nichols, 2004). These rates are spatial averages for each catchment, integrated over the residence time of quartz in the upper few meters of rock and regolith on the hillslopes ($\sim 10^4$–10^5 yr in the Appalachian Mountains) (Matmon et al., 2003). Sediment was sieved to 0.25–0.50 mm, quartz was purified, and Be was extracted at the University of Vermont using standard techniques (Kohl and Nishiizumi, 1992; Bierman and Caffee, 2001). ^{10}Be/^{9}Be ratios were measured by accelerator mass spectrometry at the Lawrence Livermore National Laboratory and normalized to the KNSTD3110 standard to calculate ^{10}Be concentrations (Reuter, 2005). Catchment-averaged ^{10}Be production rates were calculated on a pixel-by-pixel basis from a 30 m DEM by Portenga and Bierman (2011), correcting for latitude and elevation by applying the scaling schemes of Lal (1991) and Stone (2000). No corrections were made for topographic shielding, quartz enrichment, magnetic field variations, or snow cover. Erosion rates were originally reported by Reuter (2005) and updated (considering the change in ^{10}Be halflife and thus standard values of Nishiizumi et al. (2007)) by Portenga and Bierman (2011) using the CRONUS online calculator (Balco et al., 2008), and assume a rock density of 2.7 g/cm^3. Each catchment is underlain by a single dominant lithology, hence we assume quartz distribution is uniform. Larger catchments with well-defined floodplains and alluvial fans were not included in the analysis, so long-term sediment storage is likely minimal.

Along three of the tributaries, samples were collected by Reuter (2005) both upstream and downstream of knickpoints allowing us to evaluate along-stream variations in erosion rate. We deconvolved erosion rates below knickpoints using a two-component mixing model (Granger et al., 1996; see description in Online supplementary material) that specifically accounts for the areas of hillslopes above and below knickpoints following the approach of other studies (Reinhardt et al., 2007; Van den Berg et al., 2012; erosion rates modeled for the below-knickpoint areas are the bold, italicized values in Table S2).

4. Results

4.1. Stream profiles

Regional analysis shows that knickpoints are common in tributary channels of the Main Branch and West Branch Susquehanna River (Fig. 2). The 61 knickpoints identified have a mean elevation of 411 m ($1\sigma = 127$ m). This sample includes a small number (7%) between 50 and 150 m elevation; most (85%) of the remainder lies between 300 and 600 m. The low-elevation cluster of knickpoints appears to be associated with a well-studied convexity along the lower 200 km of the Susquehanna River (Pazzaglia and Gardner, 1993) that is thought to be related to flexural deformation of the Atlantic seaboard (Pazzaglia and Gardner, 1994). The higher elevation group of knickpoints spans all geologic provinces in the Susquehanna catchment; this group is the focus of the remainder of this paper.

The higher elevation knickpoints occur in diverse rock types (e.g., carbonates, clastics ranging from mudstone to conglomerate, and metamorphics including quartzite and metarhyolite) and have upstream drainage areas that range over 5 orders of magnitude (0.2–49,600 km^2; Table S1 in Online supplementary materials). These knickpoints are well defined in slope-area plots at the breaks between to two sub-parallel scaling trends reflecting ~2–3 fold differences in channel steepness (Fig. 3). Viewed together, such overlapping slope-area plots demonstrate the shared behavior among streams across the spatially large, geologically diverse region.

On the whole, mean steepness indices in these tributaries are 15 ± 2 m$^{0.9}$ above knickpoints and 43 ± 5 m$^{0.9}$ below (Fig. 3 inset). Mean concavity indices (θ) are 0.41 ± 0.06 and 0.45 ± 0.18, above and below knickpoints, respectively. This latter observation confirms that differences in channel profile gradient can be examined regionally by mapping channel steepness index. Overall, steepness indices within the Susquehanna catchment range from ~5 to ~170 m$^{0.9}$. The greatest steepness indices correspond to the lower Susquehanna River where it crosses the Piedmont and through Holtwood Gorge (Fig. 4). Other coherent regions of steep channel gradients ($k_{sn} \approx 40$ m$^{0.9}$) occur hundreds of kilometers farther upstream, immediately downstream of most of the high-elevation knickpoints that we identified. These knickpoints, in turn, lie at the downstream boundaries of low-steepness regions

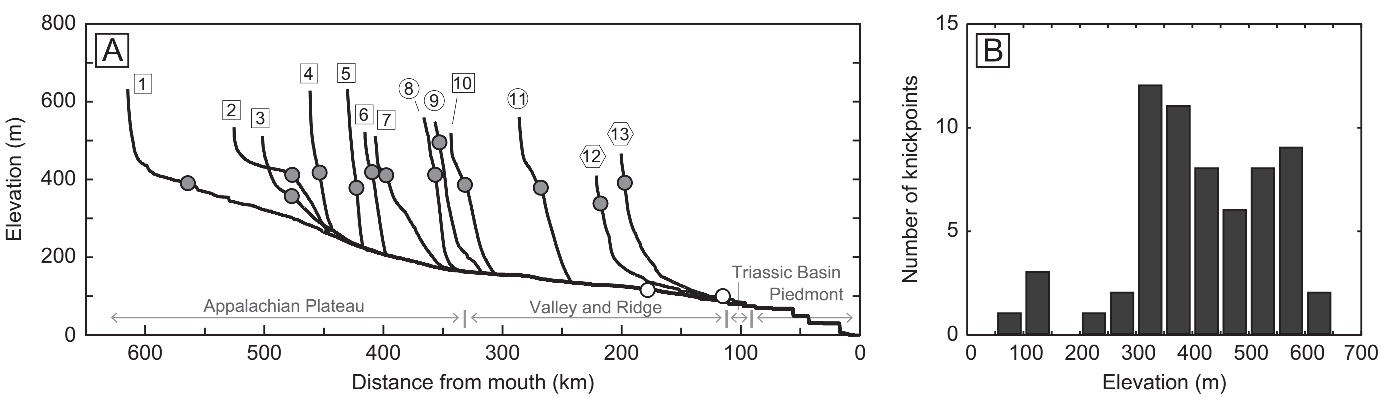

Fig. 2. Longitudinal profiles and knickpoints. (A) Representative profiles (black lines) showing low (< 200 m) and high (> 200 m) elevation knickpoints (white and gray circles, respectively). Numbered stream profiles correspond to the key in Fig. 1 caption. Shapes around numbers indicate the geologic province where the tributary and knickpoint are located (circles: Appalachian Plateau; squares: Valley and Ridge; hexagons: Blue Ridge). Geologic provinces crossed by the trunk stream are shown in gray at the bottom. (B) Histogram of knickpoint elevations identified from slope-area plots. Identification criteria described in text.

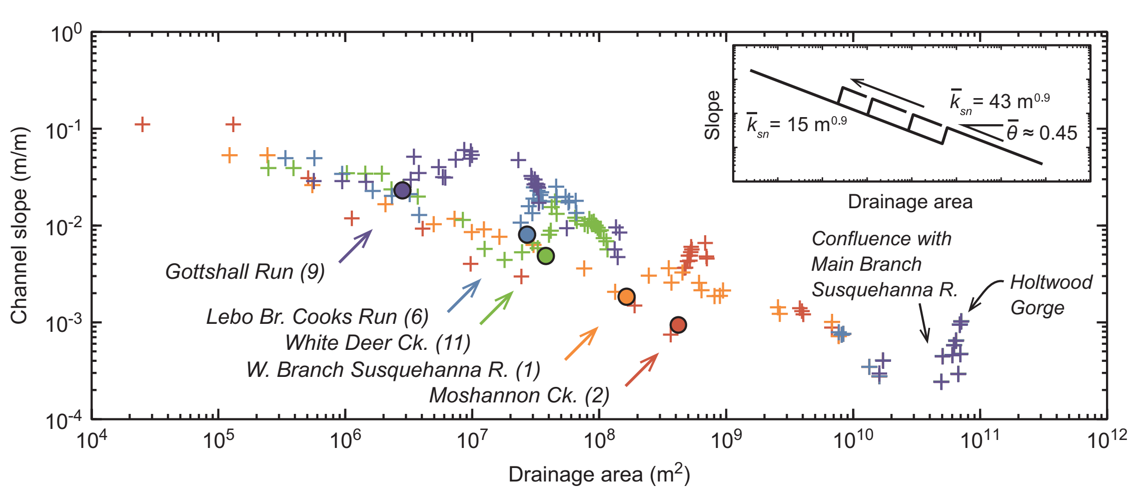

Fig. 3. Composite slope-area plot of five representative streams showing points on channel (crosses) and knickpoints (circles). Inset shows schematic overview of stream profile parameters above and below knickpoints. Lines and arrow show the transient evolution of detachment-limited stream profiles responding to base level fall (Snyder et al., 2000). Stream numbers same as Figs. 1 and 2.

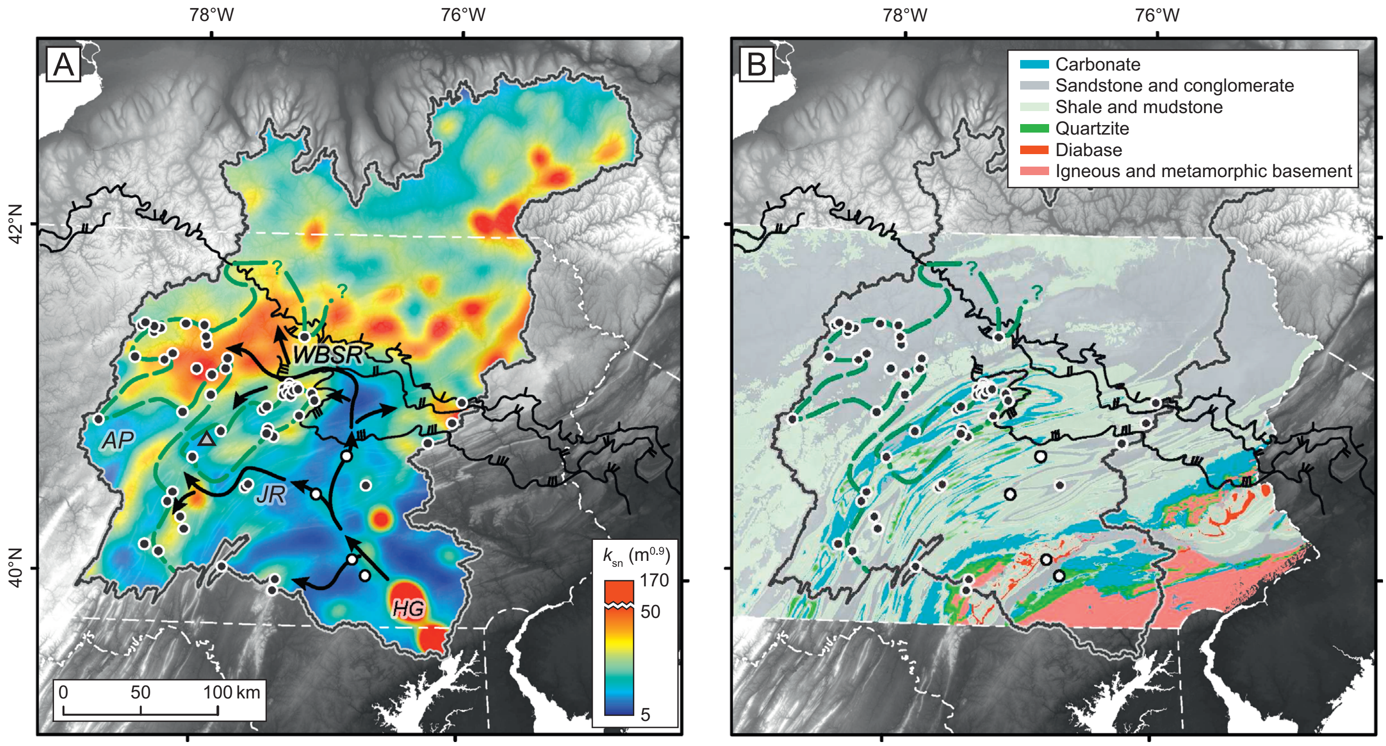

Fig. 4. Maps showing the spatial relationships between knickpoints, steepness, and lithology. (A) Map showing spatially averaged k_{sn} overlying grayscale DEM. Surface was fitted to k_{sn} calculated in 1 km segments in the channel network extracted from the 90 m DEM (following Ouimet et al. (2009); see Online supplement for further details), excluding reservoirs and dams, with a tensioned spline and smoothed with a Gaussian low-pass filter (30 km kernel width, $\sigma = 5$ km). These filter dimensions exceed the mean horizontal spacing between analyzed channels (3.5 km) and formation contacts (2.4 km), to emphasize regional trends. Black-filled circles are knickpoints with elevations > 200 m; white-filled circles are lower elevation knickpoints. Dashed green lines demarcate edges of large regions of inferred relict topography upstream of knickpoints; smaller patches of relict topography and regions north of glacial margin are not shown. Black arrows show paths of inferred knickpoint retreat following the modern stream network. Glacial margins marked as in Fig. 1. AP: Appalachian Plateau; HG: Holtwood Gorge; JR: Juniata River; WBSR: West Branch Susquehanna River. (B) Map of dominant rock types in study area in Pennsylvania (Miles and Whitfield, 2001). Knickpoints, inferred relict landscape, and glacial margin shown as in (A).

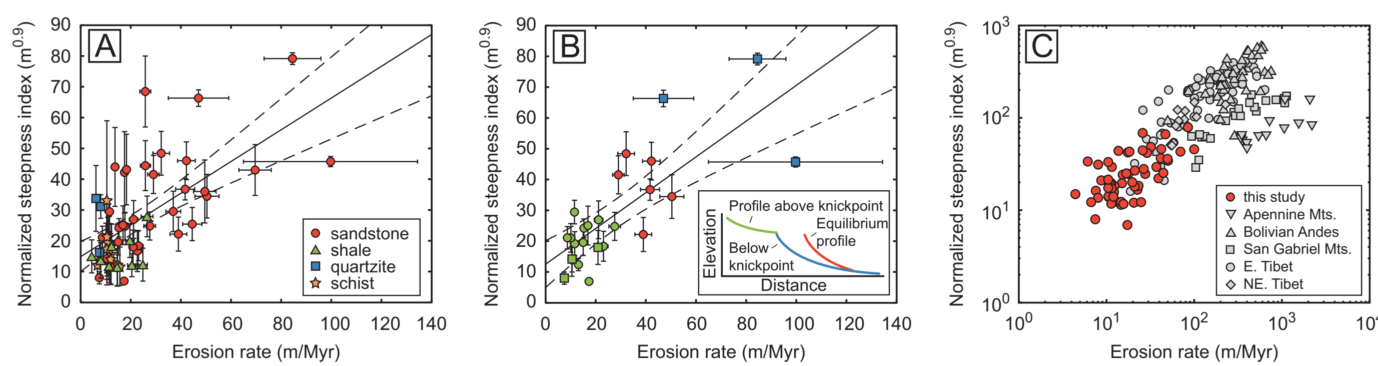

Fig. 5. Relationship between catchment-averaged normalized steepness indices, k_{sn}, and catchment-averaged erosion rates. (A) All catchments in this study, grouped by rock type. Error bars shown at 2σ level. Solid line shows linear least-squares fit; dashed lines are 95% confidence interval. $R^2 = 0.40$ with bootstrapped 95% confidence interval of 0.22–0.66. (See Table S3 in Online material for regression results.) (B) The subset of catchments that overlie sandstone and do not contain knickpoints, either because they occur upstream of knickpoints or are concave (equilibrated) tributaries downstream of knickpoints. Also shown are the three samples immediately downstream of knickpoints for which erosion rates were unmixed from paired erosion rates upstream. These three groups are color coded as shown in the inset. Squares indicate results from paired samples collected above and below knickpoints. Least-squares fit $R^2 = 0.59$, with bootstrapped 95% confidence interval, 0.36–0.85. (C) Results for all catchments in this study compared to tectonically active, nonglaciated, steady-state catchments around the world (after Kirby and Whipple (2012)). All erosion rates estimates from cosmogenic ^{10}Be inventories in river sand (Safran et al., 2005; Harkins et al., 2007; Ouimet et al., 2009; Cyr et al., 2010; DiBiase et al., 2010; Kirby and Harkins, in press). Note logarithmic axes.

on the Appalachian Plateau, as well as in high elevation valleys and broad ridge tops in the Valley and Ridge province.

4.2. Erosion rates and relationship to channel gradients

Catchment-scale erosion rates in our study, including the three deconvolved rates, range from 4 to 99 m/Myr (Table S2 in Online supplement). These rates correlate ($p < 0.01$; Table S3 in Online supplement) with channel steepness (Fig. 5A). There is no strong influence of rock type apparent in these data. Rock types other than sandstone are all eroding at rates < 30 m/Myr, but also reflect a relatively limited range of channel steepness ($k_{sn} < 35$ $m^{0.9}$). For these rock types (shale, quartzite, and schist), catchment-scale erosion rate and channel steepness do not correlate significantly; any potential differences in erodibility cannot be distinguished clearly in the data (Table S3). Thus, within the resolution available, the different rock types in our study erode equally fast at a catchment scale for a given channel steepness.

The erosion rates reported here are averaged over entire catchments, which are dominated areally by hillslopes rather than channels. However, we suggest that the channels and hillslopes are eroding at similar rates. To support this, we note the correlation ($R^2=0.70$) between hillslope gradients, represented by the mean catchment slope, and channel gradients, represented by the mean normalized steepness index (Fig. 6). This correlation is exhibited in all catchments without knickpoints, which are assumed to be in equilibrium, as well as in portions of catchments below knickpoints. This relation suggests that hillslopes are adjusted to channel gradients, even below knickpoints. This relation is also consistent with the observation that hillslope gradients in these catchments correlate well with catchment-averaged erosion rates (Reuter, 2005; Portenga and Bierman, 2011).

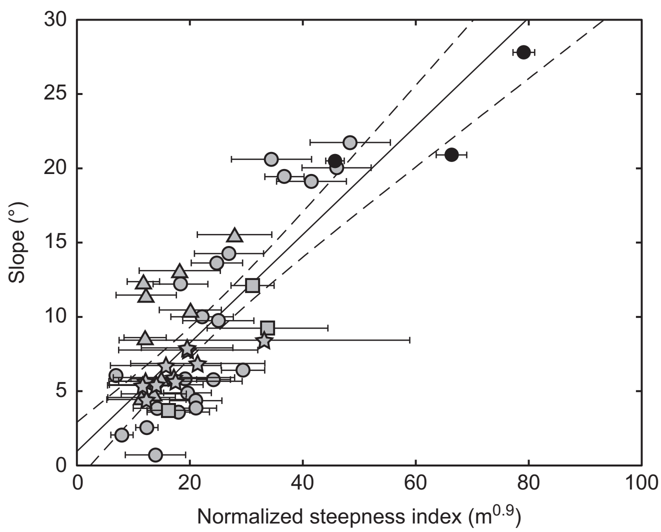

Fig. 6. The relationship between hillslope and channel gradients in different rock type (circles: sandstone; triangles: shale; squares: quartzite; stars: schist). Plot compares catchment-averaged slope against catchment-averaged normalized steepness index. Gray symbols indicate catchments without knickpoints. Black symbols represent portions of catchments below knickpoints and contiguous topographic breaks on hillslopes, for which erosion rates were deconvolved in Fig. 5.

Paired samples collected above and below knickpoints on individual tributaries, such as those shown in Fig. 7A, demonstrate that erosion rates increase immediately downstream of knickpoints by 37–78 m/Myr (samples 110–111, 120–121, and 125–126 in Table S2). In fact, most of the variance in erosion rates in our study can be explained by differences in channel steepness across knickpoints. To demonstrate this, Fig. 5B shows data for catchments in sandstone, the only rock type that was sampled both above and below knickpoints, and separates those samples according to their positions with respect to knickpoints: (1) those samples upstream of knickpoints, (2) those directly downstream of and in the same channel as knickpoints, and (3) those in concave (equilibrated) tributary channels that enter below knickpoints. Except for the three samples that allowed us to deconvolve the erosion rates below knickpoints, we excluded results from catchments that include knickpoints. Overall, sandstone catchments above knickpoints are eroding at a mean rate of 15 ± 3 m/Myr while channels and adjacent hillslopes below knickpoints, including equilibrated tributary channels and their catchments, are eroding faster at a mean rate of 52 ± 16 m/Myr.

These results indicate that spatial variations in channel gradients across the Susquehanna drainage basin largely reflect spatial variations in catchment-averaged erosion rates, conforming to the scaling relationship noted in non-glaciated, equilibrium catchments undergoing rock uplift worldwide (Fig. 5C). This latter observation, too, suggests that channel erosion rates in our study closely match catchment-averaged rates. Thus, it is reasonable to conclude that channels in the Appalachians adjust their erosion rates, and hence gradients, in response to changes in external forcing with the same physical behavior as bedrock channels in tectonically-active landscapes (Kirby and Whipple, 2012).

5. Analysis

5.1. Spatial relationships among knickpoints, channel steepness, and lithology

As noted above, erosion rates in our study show no strong sensitivity to rock type, but vary significantly across knickpoints. In this section, we broaden our analysis to the spatial association between lithology and all studied stream profiles to examine

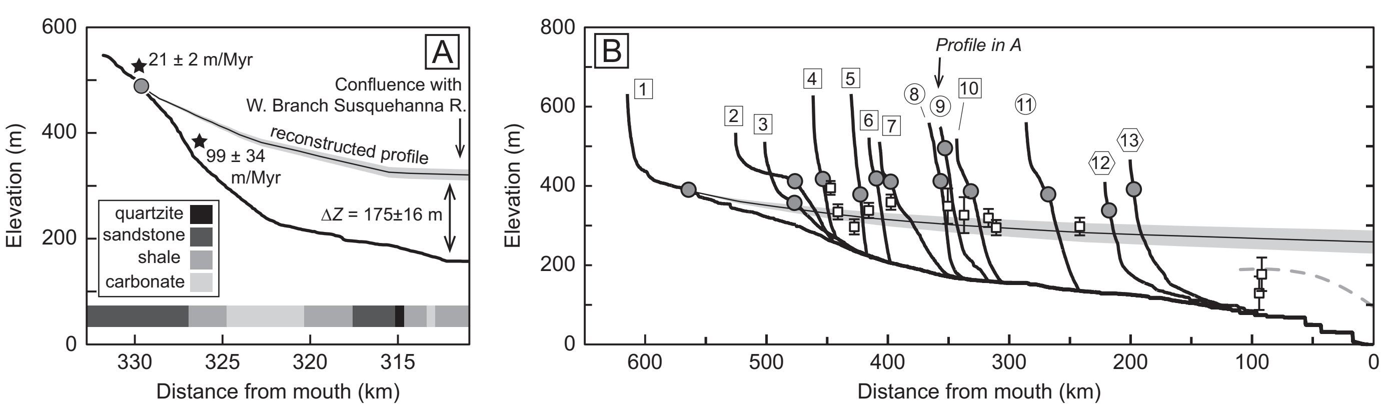

Fig. 7. Transient erosion below knickpoints. (A) Longitudinal profile of Gottshall Run, showing different erosion rates across a knickpoint (circle). Sample locations (stars) and erosion rates from ^{10}Be analysis are shown. The reconstructed relict stream profile (black dashed line) and 95% confidence interval (gray envelope) were extrapolated using the k_{sn} above the knickpoint and $\theta_{ref}=0.45$. Amount of transient channel lowering (ΔZ) at confluence with West Branch Susquehanna River is indicated. Horizontal bar below profile shows dominant rock types in formations across which the stream flows. (B) Representative longitudinal profiles with reconstructed relict profile of West Branch Susquehanna River (black dashed line) and elevations of projected relict profiles at confluences with trunk stream (squares). Errors shown at 95% confidence interval. Dashed gray line is the topographic profile of the Miocene terrace (Tg1) of Pazzaglia and Gardner (1993). Refer to Fig. 2 caption for other symbols.

whether knickpoints occur consistently with a specific rock type, or a transition from one rock type to another. The high-elevation knickpoints in our study occur in a total of 21 different lithologic formations dominated by carbonate, clastic, and metamorphic rock types and ranging in age from Precambrian to Permian (Table S1 in Online supplementary material). Steep channels below knickpoints are commonly associated with sandstone, such as on the Appalachian Plateau (Fig. 4B), but occur to lesser degrees in shale, carbonate, igneous, and metamorphic rocks (Fig. 7A; Table S1). Regions of low channel steepness above knickpoints occur in this same range of rocks (Figs. 4B and 7A). Broadly, no apparent spatial association exists between rock type and knickpoints, or rock type and channel steepness.

Nevertheless, some knickpoints could coincide with formation contacts. On average, the horizontal distance between knickpoints and the closest formation contact is 2.0 ± 0.7 km, and the mean vertical separation is 51 ± 17 m. As a whole, the sample mean does not coincide with contacts even at the 2σ level. However, 48% of individual knickpoints are separated vertically from the closest formation contact by ≤12 m, the vertical resolution of the slope-area analysis, and might therefore coincide with contacts. It remains unclear whether knickpoints are briefly detained or accentuated at these contacts, but, as large-scale features that separate portions of the landscape eroding at different rates, it is clear that they are not pinned by lithologic contrasts. We provide evidence in the next section that the knickpoints are not stationary, and thus that the role of lithology is a secondary influence on their presence and dynamics.

5.2. Comparison between observed knickpoint locations and knickpoint migration model predictions

The regionally widespread, high-elevation knickpoints in our study (1) occur across a large range of drainage areas but a limited range of elevations, (2) demarcate a systematic ~2–3 fold increase in channel steepness, and (3) are the spatial boundary between ~2 and 3 fold differences in erosion rate. Overall, these characteristics are consistent with the predicted transient response of detachment-limited channels to an increase in rock uplift rate or base level fall (Snyder et al., 2000), supported by studies from other orogens showing similarly elevated erosion rates below knickpoints (Reinhardt et al., 2007; Olivetti et al., 2012; Van den Berg et al., 2012). Knickpoint occurrence over a large range of drainage areas suggests that knickpoints do not form at a critical, small drainage area (cf. Crosby and Whipple, 2006). Instead, the cluster of knickpoint elevations follows the expectation that migratory knickpoints initiated on a single trunk stream migrate vertically through tributaries at the same rate (Niemann et al., 2001). Assuming a space-for-time substitution, these transient dynamics are represented by the overlapping slope-area plots of these streams (inset in Fig. 3).

Another way to test whether the high-elevation knickpoints are the result of transient erosion, and thus genetically related, is to examine the consistency between the locations of observed knickpoints and the locations predicted by a generic knickpoint migration model. We follow others (Crosby and Whipple, 2006; Berlin and Anderson, 2007; Whittaker and Boulton, 2012) by using an expression derived from the stream power law (see Online supplementary material), where knickpoint celerity, or dx/dt with units m/yr, is

$$dx/dt = KA^m \quad (1)$$

where K is a celerity coefficient with units of $m^{(1-2m)}$/yr, A is drainage area with units of m^2, and m is a constant that depends on erosion process, hydraulic geometry, and catchment hydrology (Whipple and Tucker, 1999). This model assumes that erodibility is not a function of sediment yield and that plucking is the primary erosion mechanism, hence erosion rate scales linearly with channel slope (Whipple et al., 2000). Given the current drainage network, for which we know the drainage area for every point, and a given combination of K and m, we solve for knickpoint position as a function of time through each tributary (Crosby and Whipple, 2006). We use a brute force approach to iterate through values of K (logarithmic increments of $10^{0.2}$ between 10^{-8} and 10^{-5} $m^{(1-2m)}$/yr) and m (increments of 0.02 between 0.40 and 0.60) to find a combination that, at time $t_{minRMSE}$, minimizes the root mean square error (RMSE) between the predicted distances of all knickpoints from the Susquehanna River mouth and the observed distances.

The resulting best fit yields a strong correlation ($R^2 = 0.98$) between predicted and observed migration distance when $m = 0.50$ and $K = 2.5 \times 10^6$ yr^{-1} at $t_{minRMSE} = 2$ Myr (Fig. 8A). For this simulation, the mean along-stream distance between observed and predicted knickpoints is only 0.3 ± 4.3 km (2σ), which is remarkably small in comparison to the individual migration distances (220–560 km) and the mean distance between observed knickpoints and the divide above their channel heads (12 ± 5 km).

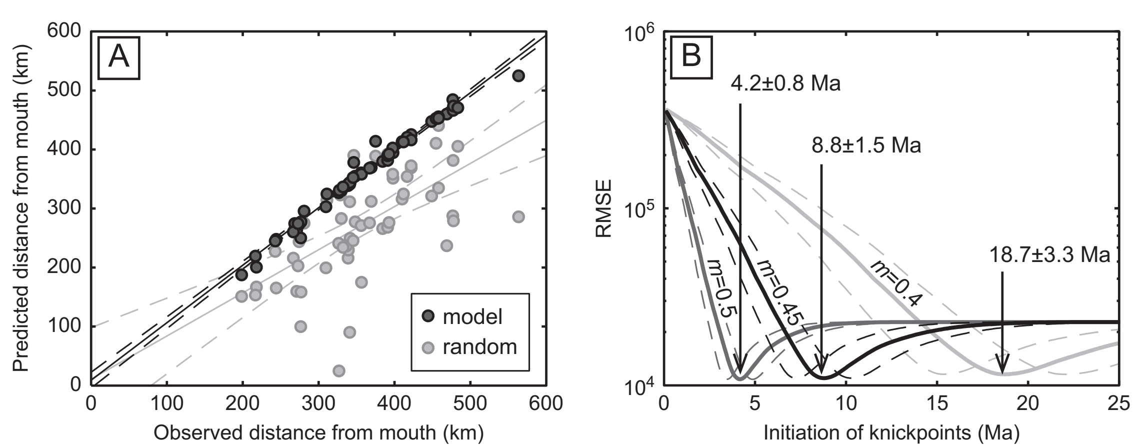

Fig. 8. Results of knickpoint migration model. (A) Plot showing the predicted distance from the river mouth for the migrating model knickpoints against the observed distance from the river mouth of real knickpoints that yields the lowest root mean square error, RMSE ($R^2 = 0.98$). For comparison, hypothetical knickpoints at random locations along each tributary are plotted against actual knickpoints ($R^2 = 0.41$). Solid lines show least-squares linear regression results; dashed lines show 95% confidence intervals. (B) Plot of RMSE between model and observed knickpoint distances from river mouth knickpoint travel time for three values of m. Solid lines represent model results using preferred celerity coefficient, K, derived from least-squares linear regression of k_{sn} and erosion rate in Fig. 5B; dashed lines represent misfits for the 95% confidence interval of K from the same regression.

Although this inverse procedure can yield a large range of similarly small misfits, and thus a large range of $t_{minRMSE}$, for different combinations of m and K (Berlin and Anderson, 2007; Gallen et al., 2013), it is not our intention to uniquely determine these parameters. Rather, this exercise demonstrates that the observed, high-elevation knickpoint positions are consistent with their being the result of a single migrating wave (arrows in Fig. 4A) of transient erosion through the existing drainage network (Bishop et al., 2005). By way of contrast, if each present-day knickpoint is instead compared to a knickpoint positioned randomly along each unique tributary (Fig. 8A), the best-fit result is poorer ($R^2 = 0.47 \pm 0.01$, mean and bootstrapped 2σ error of 1000 random samples) and the mean distance between observed and random knickpoints is larger (22.1 ± 0.5 km). Such a hypothetical scenario might be appropriate if knickpoints were (1) stationary and fixed to randomly located asperities, (2) migrating with different K but initiated concurrently, or (3) migrating with the same K but genetically unrelated. Our results suggest that none of these scenarios is likely.

5.3. *Amount of transient incision*

For streams exhibiting transient behavior but where stream terraces are absent, one approach to evaluate channel incision utilizes the steepness and concavity indices above knickpoints to project a concave profile downstream, assuming that they had concave profiles in equilibrium with prevailing conditions prior to the onset of base level fall (e.g., Goldrick and Bishop, 1995; Schoenbohm et al., 2004; Clark et al., 2005; Berlin and Anderson, 2007; Harkins et al., 2007; Kirby and Whipple, 2012; Miller et al., 2012; Morell et al., 2012; Schildgen et al., 2012; Sternai et al., 2012; Walcek and Hoke, 2012). The difference between the projected and modern channel elevations (ΔZ) is the amount of relative channel lowering, which we measure at the confluence with the Main Branch or West Branch Susquehanna River (Fig. 7A). Thirteen representative tributaries underlain by clastic rocks were reconstructed following Harkins et al. (2007) and fixing θ equal to 0.45 (Fig. 7B). The resulting projected tributary elevations nearly intersect the reconstructed trunk stream profile over a distance of ~300 km (Fig. 7B). The failure of the two reconstructed tributaries farthest downstream to intersect the trunk profile is not surprising considering that the reconstruction does not account for spatial variations in rock erodibility or crustal deformation, which has been documented by Pazzaglia and Gardner (1994) in stream terraces along the lower Susquehanna River (dashed line in Fig. 7).

Taken together, the reconstructed tributaries have been lowered at the trunk stream by an average of 128 ± 23 m (2σ error given; range: 56–180 m; Table S4 in Online supplement). This result does not account for erosion of the relict channels above knickpoints, and therefore does not account for the total base level fall over the period of transient incision. Accounting for the difference in erosion rates above (~15 ± 3 m/Myr) and below (~52 ± 16 m/Myr) knickpoints (Kirby and Whipple, 2012; Schildgen et al., 2012), the mean total base level fall is 181 ± 32 m (range: 79–264 m). Overall, tributary incision (~100–150 m) represents a modest fraction (at least 25–40%) of the local topographic relief (up to ~400 m) in the study area present today.

5.4. *Timescale of knickpoint migration*

By assuming that the relict and transient profiles are eroding at constant though different rates, one can estimate the amount of time that base level has been lowering at the tributary mouths (Kirby and Whipple, 2012; Schildgen et al., 2012). Given that the difference between mean erosion rates above and below knickpoints is 37 ± 19 m/Myr, the mean amount of time required to cause the observed tributary base level fall (128 ± 23 m) is 3.5 ± 0.6 Myr (range: 1.5–4.9 Myr; Table S4 in Online supplement).

Our calculation roughly estimates the time that transient erosion initiated along the tributaries to the Susquehanna trunk stream, but it likely underestimates the total time that migratory knickpoints have been propagating through the entire fluvial network. Although subject to model assumptions, this total migration time can be predicted by the knickpoint migration model. Assuming that erosion rate scales linearly with channel slope, the steady-state relationship between steepness index and erosion rate (E), the reciprocal of slope in Fig. 5B, can be used to constrain reasonable values of K in the knickpoint migration model (see Online supplementary information). Over a reasonable range of m (0.4–0.5) and the corresponding estimates of K, $t_{minRMSE}$ ranges from ~4 to ~19 Myr (Fig. 8B).

These estimates assume that erosion rates, as well as their relationship with channel steepness, have remained constant through time. However, it remains possible that millennial scale erosion rates estimated with cosmogenic isotopes have exceeded the Neogene average because of enhanced periglacial weathering and downslope transport during the Quaternary (Braun, 1989). Despite this uncertainty, these estimates are consistent with a number of lines of geologic evidence that suggest changes in landscape erosion and sediment flux during the late Miocene to early Pliocene. The amount of transient incision below knickpoints agrees closely with ~130 m of incision inferred from middle Miocene terraces along the lower Susquehanna River (gray dashed line in Fig. 7B; Pazzaglia and Gardner, 1993). Terrace surfaces are interpreted to correlate with coastal plain deposits (Pazzaglia, 1993), and thus incision is argued to be the cause of an increase in sediment flux and grain size to the Baltimore Canyon Trough observed at ~15 Ma (Poag and Sevon, 1989; Pazzaglia and Brandon, 1996; Steckler et al., 1999). This time period also coincided with incision into low-relief upland erosion surfaces along the New Jersey Piedmont to the east (Stanford et al., 2001; Stanford et al., 2002).

Although the magnitude of inferred Miocene denudation (1–2 km, see Pazzaglia and Brandon (1996)) in the Susquehanna drainage is large relative to our estimate, uncertainties in the source regions for offshore deposits make a direct comparison difficult. Moreover, weathering profiles present upstream of knickpoints at 280–310 m elevation in parts of the Valley and Ridge province (triangle in Fig. 4A) are thought to have formed over the past ~14 Myr (Parizek and White, 1985), suggesting that parts of the relict landscape above high-elevation knickpoints have undergone little physical erosion since middle Miocene time.

Whereas these temporal associations do not confirm that the knickpoints were initiated in the middle Miocene, it seems likely that transient incision was ongoing by late Miocene time. Continued incision along the Susquehanna River, however, maintained relatively high sediment flux to the southern Baltimore Canyon Trough through the late Miocene and Pliocene (Kulpecz et al., 2009). Incision through the Valley and Ridge province had lowered the groundwater table and initiated development of present-day cave systems by 3–5 Ma (White, 2009). Temporal comparisons are complicated by, but consistent with, the fact that transient erosion migrates upstream as a kinematic wave (Whipple and Tucker, 1999). Following middle Miocene incision, stream incision rates across the Piedmont appear to have decreased between 8 and 2 Ma to less than a third of previous rates (Pazzaglia and Gardner, 1993; Stanford et al., 2002). Proglacial lake deposits in the West Branch of the Susquehanna River indicate that the bed had lowered to its current elevation by ~1 Ma (Ramage et al., 1998), suggesting that incision rates slowed, and thus channel gradients decreased, in the wake of high-elevation knickpoints, which is consistent with the broad region of low channel steepness through the Susquehanna drainage basin at elevations of ~150–300 m (Fig. 4). Steeper channels at lower elevations, below the low-elevation set of knickpoints, may be associated with an increase in stream incision at ~2 Ma identified from the terrace record (Pazzaglia and Gardner, 1993).

6. Discussion

Our results support a growing number of studies inferring that topographic relief in the central and southern Appalachians has increased during the late Cenozoic. Such studies have been based on observations of faster millennial scale erosion rates in stream channels than on nearby ridgetops (Hancock and Kirwan, 2007; Portenga et al., 2013) and the inferred migration of knickpoints along tributary networks (Gallen et al., 2013; Prince and Spotila, in press). Our results provide the first definitive association between transient river profiles in the region and elevated erosion rates. These results argue strongly that a recent increase in topographic relief in the Susquehanna River catchment is the result of a perturbation in erosion rates propagating through the fluvial network. Moreover, the regional extent of the wave of transient incision implicates a driver that acts at wavelengths of hundreds of kilometers.

Our results are compatible with previous studies of slow exhumation in the Appalachians. Considering that Neogene incision inferred in this study from river profiles is less than a few hundred meters, similar to values observed in the central and southern Appalachians (Gallen et al., 2013), this would go largely undetected by most, if not all, low temperature thermochronologic systems (Reiners and Brandon, 2006). Moreover, the rates of incision are sufficiently low that sediment mixing from different portions of a transient fluvial network would still yield relatively slow rates of erosion. Thus, rejuvenated topography could be consistent with the observation that Quaternary erosion rates nearly match long-term exhumation rates (Matmon et al., 2003; Portenga et al., 2013). While it is clear that erosion rate data augment traditional geomorphic studies, the converse is also true: identification of transient landscapes can be critical for interpreting patterns of erosion rate data.

Factors that have been proposed to drive transient erosion and relief production in the Appalachian Mountains range from climate change, to drainage reorganization, to tectonic uplift. Topographic rejuvenation has been attributed to climate change and increased erosivity since ~4 Ma (Hancock and Kirwan, 2007), based on global increases in basin sedimentation (Zhang et al., 2001) and river incision rates (Bridgland and Westaway, 2008). However, much of the incision below high-elevation knickpoints in our study appears to predate climate change at ~4 Ma and is not easily attributed to this driver. Furthermore, faster erosion associated with channel steepening below knickpoints in our study is inconsistent with a climate-driven increase in erosivity, which should engender a reduction in channel gradients (Wobus et al., 2010).

Stream capture is a potential mechanism that can rapidly lower local base level and steepen channels in individual drainage basins. This may be a factor in the Blue Ridge province, where streams are eroding westward through the drainage divide (Harbor et al., 2005; Gunnell and Harbor, 2010; Prince et al., 2011). Similarly, drainage reorganization along the Ohio River, west of the divide, may also drive transient incision in this region (Granger et al., 2001; Prince and Spotila, in press). However, there is limited evidence for capture in the non-glaciated portion of the Susquehanna catchment (Strahler, 1945). Moreover, the model results presented above are consistent with knickpoint migration through the existing drainage network and our observation that certain knickpoints, such as in the Blue Ridge province, are relatively close to the Susquehanna outlet. Thus, any large-scale drainage reorganization of the Susquehanna River network, such as westward migration of the drainage divide proposed by Pazzaglia and Brandon (1996), must have occurred earlier than the arrival of the wave of incision identified in our study.

We suggest that transient incision (on the order of ~100–150 m) now migrating through headwater reaches of the Susquehanna catchment is the remnant of a wave of incision induced by differential epierogenic rock uplift during Neogene time. The absence of Neogene stream terraces more than 120 km upstream of the Susquehanna River mouth has been typically interpreted to suggest that the magnitude of Late Cenozoic incision declined upstream, a consequence of a flexural bulge being centered over the Piedmont province (Pazzaglia and Gardner, 1993, 1994). In contrast, our results imply that Neogene incision was widespread throughout the drainage basin and associated with a broad, regional perturbation to the landscape. Although isostatic flexure driven by continental denudation and offshore deposition may be responsible for up to ~60 m of differential rock uplift across the Valley and Ridge and Appalachian Plateau (Pazzaglia and Gardner, 2000), it appears that flexure can explain only a fraction of the base level fall observed in streams and is superimposed on a broader pattern of uplift.

Recent modeling of global flow in the mantle driven by density variations suggests that the observed late Cenozoic incision could be the result of a change in dynamic support of topography. Dynamic topography is a transient feature that drives long-wavelength, low-amplitude changes in surface topography and may engender geomorphic responses similar to those presented here (e.g., knickpoints), as well as drainage reorganization (Roberts and White, 2010; Roberts et al., 2012; Braun et al., in press). The eastern seaboard of North America was subjected to long-term dynamic subsidence as North America overrode the ancient Farallon slab (Spasojević et al., 2008; Flament et al., 2013). In some model realizations (Moucha et al., 2008), changes in this flow field over the past ~30 Ma drive ~100–200 m of surface uplift of the central Appalachians (contours in Fig. 1A). South of the study area, null shear-wave splitting results under the Piedmont and Coastal Plain provinces may indicate vertical mantle flow (Long et al., 2010; Wagner et al., 2012a), consistent with shear-wave tomography that suggests vertical ascent of volatile-rich fluids above the Farallon slab (van der Lee et al., 2008). Moreover, Oligocene to late Miocene unconformities across the Norfolk Arch and elevated mid-Pliocene shallow marine sediments on the southeastern US Coastal Plain cannot be explained by flexure of the coastal margin or eustasy (Pazzaglia and Gardner, 2000; Kulpecz et al., 2009; Rowley et al., 2011). Such geologic evidence for dynamic uplift is consistent with certain mantle flow models (Moucha et al., 2008; Rowley et al., 2011), but not with others (Spasojević et al., 2008). It is also possible that on-going subduction of the Farallon slab may be driving mantle flow that, in turn, facilitated convective removal of the lower lithosphere beneath the central Appalachians beneath the Susquehanna catchment (Moucha et al., 2012), as has been suggested in the southern Appalachians (Wagner et al., 2012b; Gallen et al., 2013).

7. Conclusions

Analysis of stream profiles throughout the Susquehanna River catchment in the central Appalachian Mountains reveals a cluster of knickpoints between elevations of 300 and 600 m that marks a regional transition from gently sloping channels upstream to steeper channels downstream. These knickpoints are present in a range of rock types and are not pinned to resistant units, challenging notions that regional topography reflects a delicate balance between erosion and rock erodibility. Moreover, erosion rates determined from cosmogenic ^{10}Be inventories scale with channel steepness and increase significantly below knickpoints, suggesting that these features are transient aspects of the channel network. This evidence points to an ongoing wave of ~100–150 m of incision that has been propagating upstream since at least 3.5 Ma, and possibly since ~15 Ma, driving relief growth over this part of the passive margin. The widespread occurrence of knickpoints, consistency in estimated incision depth throughout the unglaciated portion of the catchment, and high elevation of relict landscapes suggests this region underwent over 100 m of surface uplift in the late Cenozoic, consistent with some models of mantle-supported dynamic topography along the eastern margin of North America.

Acknowledgments

This work was partially supported by USGS EDMAP Grant 08HQAG088 (P.B.S.), NSF Grant EAR-310208 (P.R.B.), the Alexander von Humboldt Foundation (E.K.), and by the NSF Susquehanna/Shale Hills Critical Zone Observatory, Grant EAR-0725019 (E.K.). J. Reuter did the sample collection and the isotope analyses. The comments of two anonymous reviewers greatly improved this paper.

Appendix A. Supporting information

Supplementary data associated with this article can be found in the online version at http://dx.doi.org/10.1016/j.epsl.2013.04.007.

References

Balco, G., Stone, J.O., Lifton, N.A., Dunai, T.J., 2008. A complete and easily accessible means of calculating surface exposure ages or erosion rates from ^{10}Be and ^{26}Al measurements. Quat. Geochronol. 3, 174–195.
Baldwin, J.A., Whipple, K.X., Tucker, G.E., 2003. Implications of the shear stress river incision model for the timescale of postorogenic decay of topography. J. Geophys. Res. 108, 2158.
Berlin, M.M., Anderson, R.S., 2007. Modeling of knickpoint retreat on the Roan Plateau, western Colorado. J. Geophys. Res. 112, F03S06.
Bierman, P., Steig, E.J., 1996. Estimating rates of denudation using cosmogenic isotope abundances in sediment. Earth Surf. Processes Landforms 21, 125–139.
Bierman, P.R., Caffee, M., 2001. Slow rates of rock surface erosion and sediment production across the Namib Desert and escarpment, Southern Africa. Am. J. Sci. 301, 326–358.
Bierman, P.R., Nichols, K.K., 2004. Rock to sediment—slope to sea with ^{10}Be—rates of landscape change. Annu. Rev. Earth Planet. Sci. 32, 215–255.
Bishop, P., Goldrick, G., 2010. Lithology and the evolution of bedrock rivers in post-orogenic settings: constraints from the high-elevation passive continental margin of SE Australia. In: Bishop, P., Pillans, B. (Eds.), Australian Landscapes. Geological Society Publishing House, Bath, pp. 267–287.
Bishop, P., Hoey, T.B., Jansen, J.D., Artza, I.L., 2005. Knickpoint recession rate and catchment area; the case of uplifted rivers in eastern Scotland. Earth Surf. Processes Landforms 30, 767–778.
Boettcher, S.S., Milliken, K.L., 1994. Mesozoic–Cenozoic unroofing of the southern Appalachian Basin; apatite fission track evidence from Middle Pennsylvanian sandstones. J. Geol. 102, 655–668.
Braun, D.D., 1989. Glacial and periglacial erosion of the Appalachians. Geomorphology 2, 223–256.
Braun, J., Robert, X., Simon-Labric, T.Eroding dynamic topography. Geophys. Res. Lett., http://dx.doi.org/10.1002/grl.50310, in press.
Bridgland, D., Westaway, R., 2008. Climatically controlled river terrace staircases: a worldwide Quaternary phenomenon. Geomorphology 98, 285–315.
Brown, E.T., Stallard, R.F., Larsen, M.C., Raisbeck, G.M., Yiou, F., 1995. Denudation rates determined from the accumulation of in situ-produced ^{10}Be in the luquillo experimental forest, Puerto Rico. Earth Planet. Sci. Lett. 129, 193–202.
Clark, M.K., Maheo, G., Saleeby, J., Farley, K.A., 2005. The non-equilibrium landscape of the southern Sierra Nevada, California. GSA Today 15, 4–10.
Crosby, B.T., Whipple, K.X., 2006. Knickpoint initation and distribution within fluvial networks: 236 waterfalls in the Waipaoa River, North Island, New Zealand. Geomorphology 82, 16–38.
Cyr, A.J., Granger, D.E., Olivetti, V., Molin, P., 2010. Quantifying rock uplift rates using channel steepness and cosmogenic nuclide-determined erosion rates; examples from northern and southern Italy. Lithosphere 2, 188–198.
Davis, W.M., 1889. The rivers and valleys of Pennsylvania. Natl. Geogr. Mag. 1, 183–253.
DiBiase, R.A., Whipple, K.X., 2011. The influence of erosion thresholds and runoff variability on the relationships among topography, climate, and erosion rate. J. Geophys. Res. 116, F04036.
DiBiase, R.A., Whipple, K.X., Heimsath, A.M., Ouimet, W.B., 2010. Landscape form and millennial erosion rates in the San Gabriel Mountains, CA. Earth Planet. Sci. Lett. 289, 134–144.
Duvall, A., Kirby, E., Burbank, D., 2004. Tectonic and lithologic controls on bedrock channel profiles and processes in coastal California. J. Geophys. Res. 109, F04004.
Engel, S.A., Gardner, T.W., Ciolkosz, E.J., 1996. Quaternary soil chronosequences on terraces of the Susquehanna River, Pennsylvania. Geomorphology 17, 273–294.
Faill, R.T., 1998. A geologic history of the north-central Appalachians, Part 3. The Alleghany orogeny. Am. J. Sci. 298, 131–179.
Faill, R.T., 2003. The early Mesozoic Birdsboro central Atlantic margin basin in the Mid-Atlantic region, eastern United States. Geol. Soc. Am. Bull. 115, 406–421.
Flament, N., Gurnis, M., Müller, R.D., 2013. A review of observations and models of dynamic topography. Lithosphere 5, 189–210.
Flint, J.J., 1974. Stream gradient as a function of order, magnitude, and discharge. Water Resour. Res. 10, 969–973.
Frankel, K.L., Pazzaglia, F.J., Vaughn, J.D., 2007. Knickpoint evolution in a vertically bedded substrate, upstream dipping terraces, and Atlantic slope bedrock channels. Geol. Soc. Am. Bull. 119, 476–486.
Fullerton, D.S., Bush, C.A., Pennell, J.N., 2003. Map of Surficial Deposits and Materials in the Eastern and Central United States (East of 102° West Longitude), Geologic Investigations Series I-2789. United States Geological Survey.
Gallen, S.F., Wegmann, K.W., Bohnenstieh, D.R., 2013. Miocene rejuvenation of topographic relief in the southern Appalachians. GSA Today 23, 4–10.
Gallen, S.F., Wegmann, K.W., Frankel, K.F., Hughes, S., Lewis, R.Q., Lyons, N., Paris, P., Ross, K., Bauer, J.B., Witt, A.C., 2011. Hillslope response to knickpoint migration in the Southern Appalachians: implications for the evolution of post-orogenic landscapes. Earth Surf. Processes Landforms 36, 1254–1267.
Gesch, D.B., 2007. The National Elevation Dataset. In: Maune, D. (Ed.), Digital Elevation Model Technologies and Applications: The DEM Users Manual, 2nd ed. American Society for Photogrammetry and Remote Sensing, Bethesda, Maryland, pp. 99–118.
Goldrick, G., Bishop, P., 1995. Differentiating the roles of lithology and uplift in the steepening of bedrock river long profiles: an example from southeastern Australia. J. Geol. 103, 227–231.
Goldrick, G., Bishop, P., 2007. Regional analysis of bedrock stream long profiles: evaluation of Hack's SL form, and formulation and assessment of an alternative (the DS form). Earth Surf. Processes Landforms 32, 649–671.
Granger, D.E., Fabel, D., Palmer, A.N., 2001. Pliocene–Pleistocene incision of the Green River, Kentucky, determined from radioactive decay of cosmogenic ^{26}Al and ^{10}Be in Mammoth Cave sediments. Geol. Soc. Am. Bull. 113, 825–836.
Granger, D.E., Kirchner, J.W., Finkel, R., 1996. Spatially averaged long-term erosion rates measured from in situ-produced cosmogenic nuclides in alluvial sediment. J. Geol. 104, 249–257.
Granger, D.E., Kirchner, J.W., Finkel, R.C., 1997. Quaternary downcutting rate of the New River, Virginia, measured from differential decay of cosmogenic ^{26}Al and ^{10}Be in cave-deposited alluvium. Geology 25, 107–110.
Gunnell, Y., Harbor, D.J., 2010. Butte detachment; how pre-rift geological structure and drainage integration drive escarpment evolution at rifted continental margins. Earth Surf. Processes Landforms 35, 1373–1385.
Hack, J.T., 1960. Interpretation of erosional topography in humid temperate regions. Am. J. Sci. 258-A, 80–97.
Hack, J.T., 1982. Physiographic Divisions and Differential Uplift in the Piedmont and Blue Ridge. U.S. Geological Survey, Reston.
Hancock, G., Kirwan, M., 2007. Summit erosion rates deduced from ^{10}Be; implications for relief production in the Central Appalachians. Geology 35, 89–92.
Harbor, D., Bacastow, A., Heath, A., Rogers, J., 2005. Capturing variable knickpoint retreat in the central Appalachians, USA. Geogr. Fis. Dinamica Quat. 28, 23–36.
Harkins, N., Kirby, E., Heimsath, A., Robinson, R., Reiser, U., 2007. Transient fluvial incision in the headwaters of the Yellow River, northeastern Tibet, China. J. Geophys. Res. 112, F03S04.
Hickok, W.O., 1933. Erosion surfaces in south-central Pennsylvania. Am. J. Sci. 25, 101–122.
King, S.D., 2007. Hotspots and edge-driven convection. Geology 35, 223–226.
Kirby, E., Harkins, N. Distributed deformation around the eastern tip of the Kunlun fault. Int. J. Earth Sci., http://dx.doi.org/10.1007/s00531-013-0872-x, in press.
Kirby, E., Johnson, C., Furlong, K., Heimsath, A., 2007. Transient channel incision along Bolinas Ridge, California: evidence for differential rock uplift adjacent to the San Andreas fault. J. Geophys. Res. 112, F03S07.
Kirby, E., Whipple, K., 2001. Quantifying differential rock-uplift rates via stream profile analysis. Geology 29, 415–418.
Kirby, E., Whipple, K.X., 2012. Expression of active tectonics in erosional landscapes. J. Struct. Geol. 44, 54–75.
Kirby, E., Whipple, K.X., Tang, W., Chen, Z., 2003. Distribution of active rock uplift along the eastern margin of the Tibetan Plateau: inferences from bedrock river profiles. J. Geophys. Res. 108, 2217.
Kohl, C.P., Nishiizumi, K., 1992. Chemical isolation of quartz for measurement of in-situ-produced cosmogenic nuclides. Geochim. Cosmochim. Acta 56, 3583–3587.

Kulpecz, A.A., Miller, K.G., Browning, J.V., Edwards, L.E., Powars, D.S., McLaughlin, P. P., Harris, A.D., Feigenson, M.D., 2009. Postimpact deposition in the Chesapeake Bay impact structure: variations in eustasy, compaction, sediment supply, and passive-aggressive tectonism. Geol. Soc. Am. Spec. Pap. 458, 811–837.

Lal, D., 1991. Cosmic ray labeling of erosion surfaces: in situ nuclide production rates and erosion models. Earth Planet. Sci. Lett. 104, 424–439.

Long, M.D., Benoit, M.H., Chapman, M.C., King, S.D., 2010. Upper mantle anisotropy and transition zone thickness beneath southeastern North America and implications for mantle dynamics. Geochem. Geophys. Geosyst. 11, Q10012.

Matmon, A., Bierman, P.R., Larsen, J., Southworth, S., Pavich, M.J., Caffee, M.W., 2003. Temporally and spatially uniform rates of erosion in the southern Appalachian Great Smoky Mountains. Geology 31, 155–158.

Miles, C.E., Whitfield, T.G., 2001. Bedrock Geology of Pennsylvania (1:250,000). Pennsylvania Geological Survey, Harrisburg.

Miller, S.R., Baldwin, S.L., Fitzgerald, P.G., 2012. Transient fluvial incision and active surface uplift in the Woodlark Rift of eastern Papua New Guinea. Lithosphere 4, 131–149.

Mills, H.H., 2003. Inferring erosional resistance of bedrock units in the east Tennessee mountains from digital elevation data. Geomorphology 55, 263–281.

Morell, K.D., Kirby, E., Fisher, D.M., van Soest, M., 2012. Geomorphic and exhumational response of the Central American Volcanic Arc to Cocos Ridge subduction. J. Geophys. Res. 117, B04409.

Morisawa, M.E., 1962. Quantitative geomorphology of some watersheds in the Appalachian Plateau. Geol. Soc. Am. Bull. 73, 1025–1046.

Moucha, R., Forte, A.M., Mitrovica, J.X., Rowley, D.B., Quéré, S., Simmons, N.A., Grand, S.P., 2008. Dynamic topography and long-term sea-level variations: there is no such thing as a stable continental platform. Earth Planet. Sci. Lett. 271, 101–108.

Moucha, R., Rowley, D.B., Levin, V.L., Simmons, N.A., Forte, A.M., 2012. Convective Removal of the Northeastern Portion of the North-American Tectospheric Root and the Late Cenozoic Uplift of the Appalachians. Eos Trans. AGU, Fall Meeting Supplement, Abstract T11B-2566.

Niemann, J.D., Gasparini, N.M., Tucker, G.E., Bras, R.L., 2001. A quantitative evaluation of Playfair's law and its use in testing long-term stream erosion models. Earth Surf. Processes Landforms 26, 1317–1332.

Nishiizumi, K., Imamura, M., Caffee, M.W., Southon, J.R., Finkel, R.C., McAninch, J., 2007. Absolute calibration of ^{10}Be AMS standards. Nucl. Instrum. Methods Phys. Res. Sect. B: Beam Interact. Mater. Atoms 258, 403–413.

Olivetti, V., Cyr, A.J., Molin, P., Faccenna, C., Granger, D.E., 2012. Uplift history of the Sila Massif, southern Italy, deciphered from cosmogenic ^{10}Be erosion rates and river longitudinal profile analysis. Tectonics 31, TC3007.

Ouimet, W.B., Whipple, K.X., Granger, D.E., 2009. Beyond threshold hillslopes: channel adjustment to base-level fall in tectonically active mountain ranges. Geology 37, 579–582.

Parizek, R.R., White, W.B., 1985. Application of Quaternary and Tertiary Geological Factors to Environmental Problems in Central Pennsylvania. Field Conference of Pennsylvania Geologists. 50th Annual Field Conference Guidebook, State College, Pennsylvania. pp. 63–119.

Pazzaglia, F.J., 1993. Stratigraphy, petrography, and correlation of late Cenozoic middle Atlantic Coastal Plain deposits: implications for late-stage passive-margin geologic evolution. Geol. Soc. Am. Bull. 106, 1617–1634.

Pazzaglia, F.J., Brandon, M.T., 1996. Macrogeomorphic evolution of the post-Triassic Appalachian Mountains determined by deconvolution of the offshore based sedimentary record. Basin Res. 8, 255–278.

Pazzaglia, F.J., Braun, D.D., Pavich, M., Bierman, P., Potter, N., Merritts, D., Walter, R., Germanoski, D., 2006. Rivers, glaciers, landscape evolution, and active tectonics of the central Appalachians, Pennsylvania and Maryland. In: Pazzaglia, F.J. (Ed.), Excursions in Geology and History: Field Trips in the Middle Atlantic States: Geological Society of America Field Guide 8. Geological Society of America, Boulder, Colorado, pp. 169–197.

Pazzaglia, F.J., Gardner, T.W., 1993. Fluvial terraces of the lower Susquehanna River. Geomorphology 8, 83–113.

Pazzaglia, F.J., Gardner, T.W., 1994. Late Cenozoic flexural deformation of the middle U.S. Atlantic passive margin. J. Geophys. Res. 99, 12143–112157.

Pazzaglia, F.J., Gardner, T.W., 2000. In: Summerfield, M.A. (Ed.), Late Cenozoic Landscape Evolution of the US Atlantic Passive Margin; Insights into a North American Great Escarpment. John Wiley & Sons, Chichester, pp. 283–302.

Poag, C.W., Sevon, W.D., 1989. A record of Appalachian denudation in postrift Mesozoic and Cenozoic sedimentary deposits of the U.S. Middle Atlantic continental margin. Geomorphology 2, 119–157.

Portenga, E.W., Bierman, P.R., 2011. Understanding Earth's eroding surface with ^{10}Be. GSA Today 21, 4–10.

Portenga, E.W., Bierman, P.R., Rizzo, D.M., Rood, D.H., 2013. Low rates of bedrock outcrop erosion in the central Appalachian Mountains inferred from in situ ^{10}Be. Geol. Soc. Am. Bull. 125, 201–215.

Prince, P.S., Spotila, J.A. Evidence of transient topographic disequilibrium in a landward passive margin river system: knickpoints and paleo-landscapes of the New River basin, southern Appalachians. Earth Surf. Processes Landforms, http://dx.doi.org/10.1002/esp.3406, in press.

Prince, P.S., Spotila, J.A., Henika, W.S., 2010. New physical evidence of the role of stream capture in active retreat of the Blue Ridge Escarpment, Southern Appalachians. Geomorphology 123, 305–319.

Prince, P.S., Spotila, J.A., Henika, W.S., 2011. Stream capture as driver of transient landscape evolution in a tectonically quiescent setting. Geology 39, 823–826.

Ramage, J.M., Gardner, T.W., Sasowsky, I.D., 1998. Early Pleistocene glacial Lake Lesley, west branch Susquehanna River valley, central Pennsylvania. Geomorphology 22, 19–37.

Reiners, P.W., Brandon, M.T., 2006. Using thermochronology to understand orogenic erosion. Annu. Rev. Earth Planet. Sci. 34, 419–466.

Reinhardt, L.J., Bishop, P., Hoey, T.B., Dempster, T.J., Sanderson, D.C.W., 2007. Quantification of the transient response to base-level fall in a small mountain catchment: Sierra Nevada, southern Spain. J. Geophys. Res. 112, F03S05.

Reusser, L.J., Bierman, P.R., Pavich, M.J., Zen, E., Larsen, J., Finkel, R.C., 2004. Rapid late Pleistocene incision of Atlantic passive-margin river gorges. Science 305, 499–502.

Reuter, J., 2005. Erosion Rates and Patterns Inferred from Cosmogenic ^{10}Be in the Susquehanna River Basin (M.S. Thesis). University of Vermont.

Roberts, G.G., Paul, J.D., White, N., Winterbourne, J., 2012. Temporal and spatial evolution of dynamic support from river profiles: a framework for Madagascar. Geochem. Geophys. Geosyst. 13, Q04004.

Roberts, G.G., White, N., 2010. Estimating uplift rate histories from river profiles using African examples. J. Geophys. Res. 115, B02406.

Rowley, D.B., Forte, A.M., Moucha, R., Mitrovica, J.X., Simmons, N.A., Grant, S.P., 2011. Mantle dynamic impact on passive margin evolution: implications for their architecture and derived sea level histories. In: Friedrich, A. (Ed.), Fragile Earth: Geological Processes from Global to Local Scales and Associated Hazards. Geological Society of America, Boulder, Colorado, pp. A3.

Safran, E.B., Bierman, P.R., Aalto, R., Dunne, T., Whipple, K.X., Caffee, M.W., 2005. Erosion rates driven by channel network incision in the Bolivian Andes. Earth Surf. Processes Landforms 30, 1007–1024.

Sasowsky, I.D., White, W.B., Schmidt, V.A., 1995. Determination of stream-incision rate in the Appalachian plateaus by using cave-sediment magnetostratigraphy. Geology 23, 415–418.

Scharf, T.E., Codilean, A.T., de Wit, M., Jansen, J.D., Kubik, P.W., 2013. Strong rocks sustain ancient postorogenic topography in southern Africa. Geology 41, 331–334.

Schildgen, T.F., Cosentino, D., Bookhagen, B., Niedermann, S., Yıldırım, C., Echtler, H., Wittmann, H., Strecker, M.R., 2012. Multi-phased uplift of the southern margin of the Central Anatolian plateau, Turkey: a record of tectonic and upper mantle processes. Earth Planet. Sci. Lett., 317–318; 85–95.

Schoenbohm, L.M., Whipple, K.X., Burchfiel, B.C., Chen, L., 2004. Geomorphic constraints on surface uplift, exhumation, and plateau growth in the Red River region, Yunnan Province, China. Geol. Soc. Am. Bull. 116, 895–909.

Schultz, C.H., 1999. The Geology of Pennsylvania. Pennsylvania Geological Survey and Pittsburg Geological Society, Harrisburg, Pennsylvania888.

Sklar, L., Dietrich, W.E., 1998. River longitudinal profiles and bedrock incision models; stream power and the influence of sediment supply. In: Tinkler, K., Wohl, E. (Eds.), Rivers over Rock; Fluvial Processes in Bedrock Channels. American Geophysical Union, Washington, DC, pp. 237–260.

Snyder, N.P., Whipple, K.X., Tucker, G.E., Merritts, D.J., 2000. Landscape response to tectonic forcing: digital elevation model analysis of stream profiles in the Mendocino triple junction region, northern California. Geol. Soc. Am. Bull. 112, 1250–1263.

Spasojević, S., Liu, L., Gurnis, M., Müller, R.D., 2008. The case for dynamic subsidence of the U.S. east coast since the Eocene. Geophys. Res. Lett. 35, L08305.

Spotila, J.A., Bank, G.C., Reiners, P.W., Naeser, C.W., Naeser, N.D., Henika, B.S., 2004. Origin of the Blue Ridge escarpment along the passive margin of Eastern North America. Basin Res. 16, 41–63.

Springer, G.S., Kite, J.S., Schmidt, V.A., 1997. Cave sedimentation, genesis, and erosional history in the Cheat River canyon, West Virginia. Geol. Soc. Am. Bull. 109, 524–532.

Stanford, S.D., Ashley, G.M., Brenner, G.J., 2001. Late Cenozoic fluvial stratigraphy of the New Jersey Piedmont: a record of glacioeustasy, planation, and incision on a low-relief passive margin. J. Geol. 109, 265–276.

Stanford, S.D., Ashley, G.M., Russell, E.W.B., Brenner, G.J., 2002. Rates and patterns of late Cenozoic denudation in the northernmost Atlantic Coastal Plain and Piedmont. Geol. Soc. Am. Bull. 114, 1422–1437.

Steckler, M.S., Mountain, G.S., Miller, K.G., Christie-Blick, N., 1999. Reconstruction of Tertiary progradation and clinoform development on the New Jersey passive margin by 2-D backstripping. Mar. Geol. 154, 399–420.

Sternai, P., Herman, F., Champagnac, J.D., Fox, M., Salcher, B., Willett, S.D., 2012. Pre-glacial topography of the European Alps. Geology 40, 1067–1070.

Stone, J.O., 2000. Air pressure and cosmogenic isotope production. J. Geophys. Res. 105, 23753–23759.

Strahler, A.N., 1945. Hypotheses of stream development in the folded Appalachians of Pennsylvania. Geol. Soc. Am. Bull. 56, 45–88.

Van den Berg, F., Schlunegger, F., Akcar, N., Kubik, P., 2012. ^{10}Be-derived assessment of accelerated erosion in a glacially conditioned inner gorge, Entlebuch, Central Alps of Switzerland. Earth Surf. Processes Landforms 37, 1176–1188.

van der Lee, S., Regenauer-Lieb, K., Yuen, D.A., 2008. The role of water in connecting past and future episodes of subduction. Earth Planet. Sci. Lett. 273, 15–27.

Vogt, P.R., 1991. Bermuda and Appalachian-Labrador rises: common non-hotspot processes? Geology 19, 41–44.

Wagner, L.S., Long, M.D., Johnston, M.D., Benoit, M.H., 2012a. Lithospheric and asthenospheric contributions to shear-wave splitting observations in the southeastern United States. Earth Planet. Sci. Lett. 341, 128–138.

Wagner, L.S., Stewart, K., Metcalf, K., 2012b. Crustal-scale shortening structures beneath the Blue Ridge Mountains, North Carolina, USA. Lithosphere 4, 242–256.

Walcek, A.A., Hoke, G.D., 2012. Surface uplift and erosion of the southernmost Argentine Precordillera. Geomorphology 153, 156–168.

Ward, D.J., Spotila, J.A., Hancock, G.S., Galbraith, J.M., 2005. New constraints on the late Cenozoic incision history of the New River, Virginia. Geomorphology 72, 54–72.

Westaway, R., 2007. Late Cenozoic uplift of the eastern United States revealed by fluvial sequences of the Susquehanna and Ohio systems: coupling between surface processes and lower-crustal flow. Quat. Sci. Rev. 26, 2823–2843.

Whipple, K.X., 2009. The influence of climate on the tectonic evolution of mountain belts. Nat. Geosci. 2, 97–104.

Whipple, K.X., Hancock, G.S., Anderson, R.S., 2000. River incision into bedrock: mechanics and relative efficacy of plucking, abrasion, and cavitation. Geol. Soc. Am. Bull. 112, 490–503.

Whipple, K.X., Tucker, G.E., 1999. Dynamics of the stream-power river incision model: implications for height limits of mountain ranges, landscape response timescales, and research needs. J. Geophys. Res. 104, 17661–17674.

White, W.B., 2009. The evolution of Appalachian fluviokarst: competition between stream erosion, cave development, surface denudation, and tectonic uplift. J. Cave Karst Stud. 71, 159–167.

Whittaker, A.C., Boulton, S.J., 2012. Tectonic and climatic controls on knickpoint retreat rates and landscape response times. J. Geophys. Res. 117, F02024.

Wobus, C., Whipple, K.X., Kirby, E., Snyder, N., Johnson, J., Spyropolou, K., Crosby, B., Sheehan, D., 2006a. Tectonics from topography: procedures, promise, and pitfalls. In: Willett, S.D., Hovius, N., Brandon, M.T., Fisher, D. (Eds.), Tectonics, Climate, and Landscape Evolution. Geological Society of America, Boulder, Colorado, pp. 55–74.

Wobus, C.W., Crosby, B.T., Whipple, K.X., 2006b. Hanging valleys in fluvial systems; controls on occurrence and implications for landscape evolution. J. Geophys. Res. 111, F02017.

Wobus, C.W., Tucker, G.E., Anderson, R.S., 2010. Does climate change create distinctive patterns of landscape incision? J. Geophys. Res. 115, F04008.

Wolin, E., Stein, S., Pazzaglia, F., Meltzer, A., Kafka, A., Berti, C., 2012. Mineral, Virginia, earthquake illustrates seismicity of a passive-aggressive margin. Geophys. Res. Lett. 39, L02305.

Zhang, P., Molnar, P., Downs, W.R., 2001. Increased sedimentation rates and grain sizes 2–4 Myr ago due to the influence of climate change on erosion rates. Nature 410, 891–897.